Electronic Supplementary Material (ESI) for Energy & Environmental Science.
This journal is © The Royal Society of Chemistry 2015

Supporting Information

Energy Saving Electrochromic Windows by Bistable Low-HOMO level Conjugated Polymers

*Haijin Shin, Seogjae Seo, Chihyun Park, Jongbeom Na, Minsu Han, Eunkyoung Kim**

Active Polymer Center for Pattern Integration, Department of Chemical and Biomolecular Engineering, Yonsei University, 50 Yonsei-ro, Seodaemun-gu, Seoul 03722, South Korea

Fax: +82-2-312-6401; Tel: +82-2-2123-5752;

E-mail: eunkim@yonsei.ac.kr

Experimental section

Instrumentation

Proton nuclear magnetic resonance (^{1}H NMR) and Carbon nuclear magnetic resonance (^{13}C NMR) spectra were recorded on a Bruker Biospin DPX250 (250MHz) and a Bruker Biospin Avance II (400MHz) spectrometer. All the electrochemical studies were performed using a universal potentiostat [model CHI 624B (CH Instruments, Inc.)]. Optical properties were obtained on a PerkinElmer Lambda750 UV/Vis/NIR Spectrophotometer. The film thickness was measured by an Alpha-Step IQ (Tencor Instruments). SEM images were obtained on a JEOL-JSM-7001F.

Synthesis

2-(Chloromethyl)-2,3-dihydrothieno[3,4-b][1,4]dioxine The synthesis of a monomer for PE-Cl is presented in Figure 1a. 3,4-Dimethoxythiophene (1 g, 6.9 mmol) was dissolved in anhydrous toluene 100 ml) and then 3-chloropropane-1,2-diol (3.8 g, 34.7 mmol, 5 eq.) and the *p*-toluene sulfonic acid monohydrate (*p*-TSA) (0.13 g, 0.69 mmol) was added to the solution. The product mixture was stirred for 3 days at 80°C. Toluene was evaporated and product was washed with water. Then, the mixture was extracted with methylene chloride, dried over anhydrous magnesium sulfate ($MgSO_4$), and concentrated. The crude product was purified by column chromatography (hexane:methylene chloride = 3:1) and concentrated to obtain of solid product (1.1 g, 84 %). ^1H NMR (250 MHz, $CDCl_3$) : 6.32 (s, 2H), 4.50-4.11 (m, 3H), 3.88-3.64 (m, 2H). ^{13}C NMR (100MHz, $CDCl_3$) δ 141.28, 100.30, 73.00, 65.72, 41.47.

3,4-Dihydro-3,3-dimethyl-2H-thieno[3,4-b][1,4]dioxepine The synthesis of a monomer for PR-Me is presented in Figure 1a. 3,4-Dimethoxythiophene (1 g, 6.9 mmol) was dissolved in anhydrous toluene (100 ml) and then 2,2-dimethylpropane-1,3-diol (7.2 g, 69 mmol, 10 eq.) and *p*-TSA (0.13 g, 0.69 mmol) was added to the solution. The mixture was stirred for 3 days at 80°C. Toluene was evaporated and product was washed with water. Then, the mixture was extracted with methylene chloride, dried over anhydrous magnesium sulfate ($MgSO_4$), and concentrated. The crude product was purified by column chromatography (hexane : methylene chloride = 3:2) and concentrated to obtain 0.6 g of solid at a yield of 48 %. ^1H NMR (250 MHz, $CDCl_3$) : 6.49 (s, 2H), 3.73 (s, 4H), 1.03 (s, 6H). ^{13}C NMR (100MHz, $CDCl_3$) δ 150.12, 105.64, 80.22, 39.01, 21.80.

3,3-Bis(bromomethyl)-3,4-dihydro-2H-thieno[3,4-b][1,4]dioxepine The synthesis of a monomer for PR-Br is presented in Figure 1a. 3,4-Dimethoxythiophene (1 g, 6.9 mmol) was dissolved in anhydrous toluene (100ml) and then 2,2-bis(bromomethyl)propane-1,3-diol (2 g, 7.6 mmol, 1.1 eq.) and *p*-TSA (0.13 g, 0.69 mmol) was added to the solution. The mixture was stirred for 3 days at 80°C. Toluene was evaporated and product was washed with water. Then, the mixture was extracted with methylene chloride, dried over anhydrous magnesium sulfate ($MgSO_4$), and concentrated. The crude product was purified by column chromatography (hexane : methylene chloride = 3:1) and concentrated to obtain a solid product (1.9g, 80%). ^1H NMR (250 MHz, $CDCl_3$) : 6.49 (s, 2H), 4.18 (s, 4H), 3.56 (s, 4H). ^{13}C NMR (100MHz, $CDCl_3$) δ 148.78, 105.89, 74.27, 46.32, 34.55.

3,4-Dihydro-3,3-bis(methoxymethyl)-2H-thieno[3,4-b][1,4]dioxepine The synthesis of a monomer for PR-MeO is presented in Figure 1a. A 250 ml single-neck round bottom flask was filled with 50 mL of anhydrous DMF, NaH (60% in mineral oil) (0.4 g, 17.5 mmol) and methanol (0.47 ml, 11.7 mmol). The mixture was heated at 90 °C over a period of 3 hours, and then 3,3-bis(bromomethyl)-3,4-dihydro-2H-thieno[3,4-b][1,4]dioxepine (1 g, 2.9 mmol) was added in portions to the hot reagent. After stirring for 24 hours at 95 °C, the reaction mixture was cooled to room temperature added to a brine solution and extracted with diethyl ether. The organic phase was washed with water and dried over magnesium sulfate ($MgSO_4$), and the solvent was removed leaving a brown oil. The resultant oil product was purified by column chromatography on silica with hexane: dichloromethane (3:2) as the eluent to obtain a clear oil product (0.5 g, 70%). ^1H NMR (250 MHz, $CDCl_3$) : 6.45 (s, 2H), 4.01 (s, 4H), 3.46 (s, 2H), 3.23 (s, 6H). ^{13}C NMR (100MHz, $CDCl_3$) δ 149.62, 105.18, 73.53, 71.91, 59.59, 47.66.

3,3-Bis((2-ethylhexyloxy)methyl)-3,4-dihydro-2H-thieno[3,4-b][1,4]dioxepine The synthesis of a monomer for PR-EHO is presented in Figure 1a. A 250 ml single-neck round bottom flask was filled with 50 mL of anhydrous DMF, NaH (60% in mineral oil) (0.4 g, 17.5 mmol) and 2-Ethylhexanol (1.8 ml, 11.7 mmol). The mixture was heated at 90 °C for 3 hours, and then 3,3-bis(bromomethyl)-3,4-dihydro-2H-thieno[3,4-b][1,4]dioxepine (1 g, 2.9 mmol) was added stepwise to the hot reagent. After stirring for 24 hours at 95 °C, the reaction mixture was cooled to room temperature added to brine and extracted with diethyl ether. The organic phase was washed with water and dried over magnesium sulfate ($MgSO_4$) and the solvent was removed to afford a brown oil. The resulting oily product was further purified by column chromatography on silica with hexane/dichloromethane (3:2) as the eluent to obtain 3,3-bis((2-ethylhexyloxy)methyl)-3,4-dihydro-2H-thieno[3,4-b][1,4]dioxepine (0.94 g, 73% yield). ^1H NMR (250 MHz, $CDCl_3$) : 6.48 (s, 2H), 4.07 (s, 4H), 3.57 (s, 4H), 3.32 (d, 4H), 1.38-1.15 (m, 18H), 0.83 (m, 12H). ^{13}C NMR (100MHz, $CDCl_3$) δ 149.84, 105.06, 74.43, 73.91, 69.98, 48.02, 39.75, 30.81, 29.27, 24.15, 23.24, 14.25, 11.29.

Preparation of the solution for the solution Casting Polymerization (SCP)

Iron (III) chloride hexahydrate (0.3 g) was dissolved in 0.8 g of butanol and sonicated for 5 min at room temperature. To this solution, 0.2 g poly(ethylene glycol)-*block*-poly(propylene glycol)-*block*-poly(ethylene glycol) (M_n ~ 2800) was added, and the solution was sonicated for 5 min. The proper amount of a monomer was added to this oxidant solution, which was then sonicated for 1 min. Then, the above solution was filtered through a hydrophilic syringe filter and spin-coated onto the substrates while controlling the spinning speed (1200-1700 rpm) to achieve a desired film thickness of 160 nm to 250 nm. After the coating process, the solution-coated substrate was heated to 50–60 °C to trigger the oxidative polymerization, producing a colored polymeric film on the substrate. After cooling to room temperature, the conductive polymer-coated substrate was washed with isopropyl alcohol or ethanol to remove any residual oxidant, low molecular weight oligomers, and impurities. After washing the substrate, the film was dried under N_2 flow and used in the electrochromic devices.

Fabrication of the Electrochromic Window(ECW)

A 2.5-cm^2 ECW was prepared using the CPs coated with ITO (the working electrode) and with bare ITO (the counter electrode). The space (100 μm) between the two electrodes was controlled by placing Surlyn (Thermoplastic resins, DuPont) as a spacer and adhesive. The electrolyte solution was injected into the sandwiched electrodes with two holes as the inlet and outlet, and the holes were then sealed with silicone sealant (Shin-Etsu).

Ultraviolet photoelectron spectroscopy (UPS)

UPS were obtained with He (I) excitation of 21.2 eV (Tilt : 90°, Bias : -7.0eV, Pass energy : 0.59eV, Neutralizer off). UPS spectra were for CPs (~10nm) on ITO substrates. Vertical black solid lines of the spectra represent onset of π- bands. A slight shift observed depending on the CPs with different functional group.

The electrochemical impedance spectral (EIS) measurements

Randles equivalent circuit was used to fit the impedance data. The parameters of the equivalent circuit included the ohmic resistance of the bulk solution (R_S), the charge transfer resistance (R_{ct}); the resistance of the charge transfer across the surface, the Warburg impedance (Z_W) resulting from the diffusive resistance and the double layer capacitance (C_{dl}). The capacitances of the ILs were determined from an impedance analyzer (Ivium B08016, Ivium technology) as a function of frequency (from 100kHz to 48 Hz, signal amplitude: 20 mV) using simulation software (Zview 2.8d, Scribner Associates Inc.). A 100μm thick IL layer was sandwiched between the bare ITO electrodes (surface resistivity 15-25 Ω/sq) and CPs coated ITO electrode. The Nyquist plot of bleached CPs exhibited the partial small semicircle portion at higher frequencies which corresponds to the charge transfer resistance whereas the line at lower frequencies which represent the diffusion limited charge transfer process (Figure S6a). In the colored state of CPs, on the other hand, semicircle portion at higher frequencies turns into a nearly straight line. It indicates that charge transfer accelerated (Figure S6b). The decrease charge transfer resistance in colored state was found to be ~77% compared to the bleached state and is attributed to the multilayer that play retarding the transfer of charges.

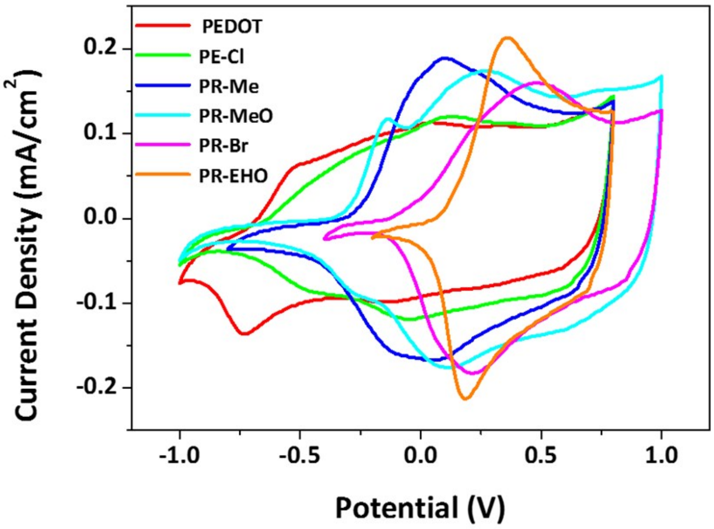

Fig. S1. Cyclic voltammograms of the CPs coated on an ITO in BIL (electrolyte) at a scan rate of 50 mV s^{-1} (V vs. Ag/AgCl) for PEDOT (red), PE-Cl (green), PR-Me (blue), PR-MeO (cyan), PR-Br (magenta), and PR-EHO (orange).

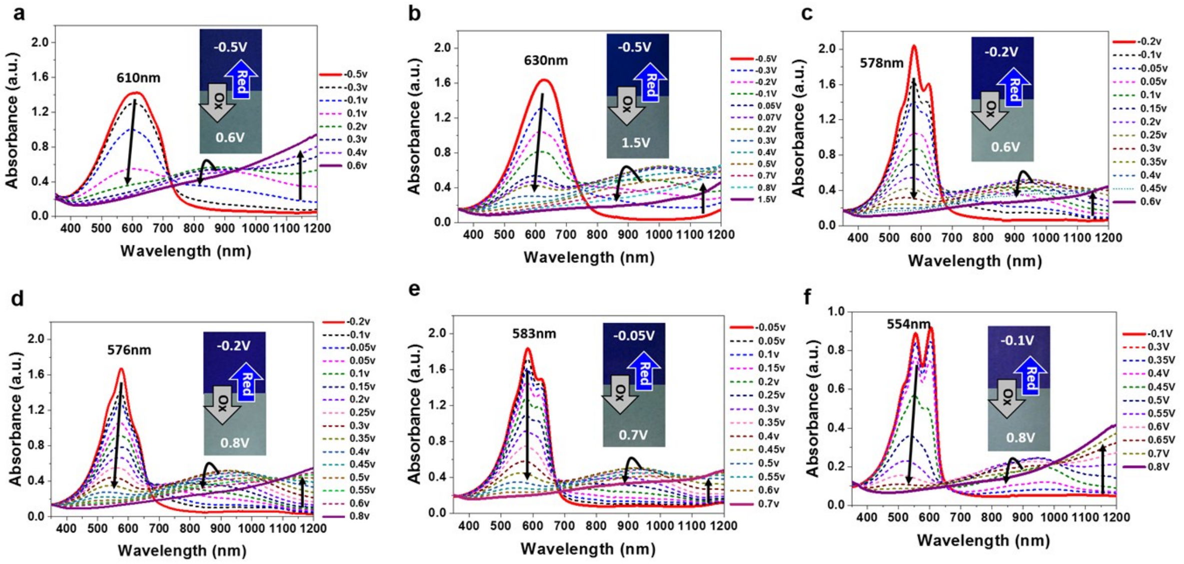

Fig. S2. In situ spectroelectrochemistry. Electrochemical oxidation of the films was performed in TABP using Ag/AgCl and a stainless flag as the counter electrode. (**a**) PEDOT (**b**) PE-Cl. (**c**) PR-Me. (**d**) PR-MeO. (**e**) PR-Br. (**f**) PR-EHO.

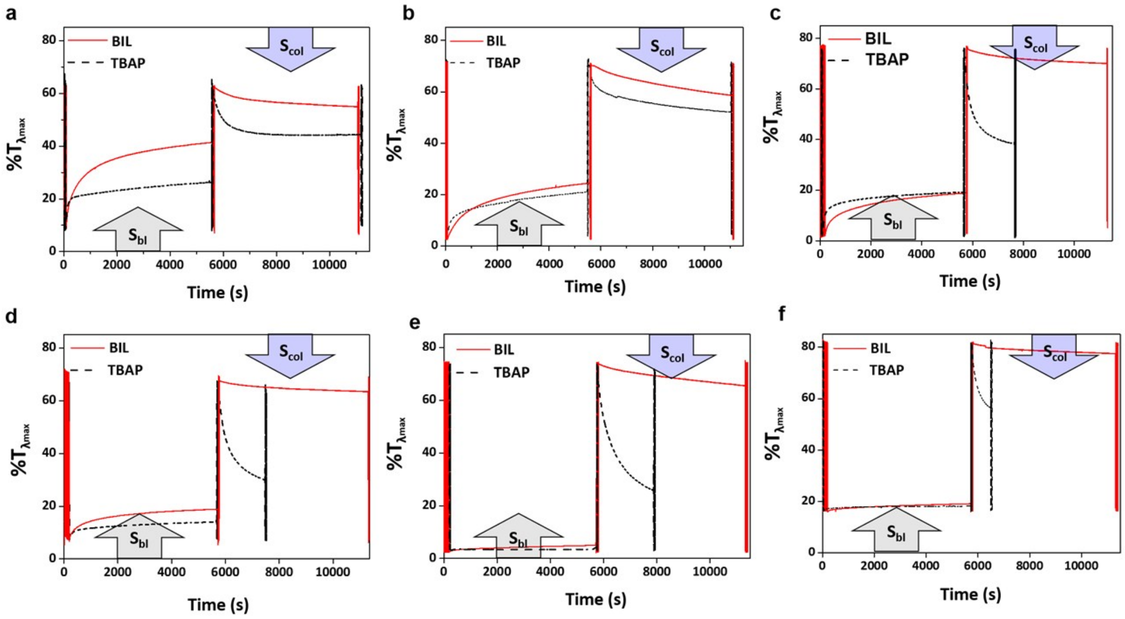

Fig. S3. The OM of the ECWs at λ_{max} in TBAP (dotted black line) and BIL (solid red line). (**a**) PEDOT (±3.3 V / 610 nm). (**b**) PE-Cl (±3.3 V / 630 nm). (**c**) PR-Me (±2.8 V / 578 nm). (**d**) PR-MeO (±2.8 V / 576 nm). (**e**) PR-Br (±2.8 V / 583 nm). (**f**) PR-EHO (±2.8 V / 554 nm).

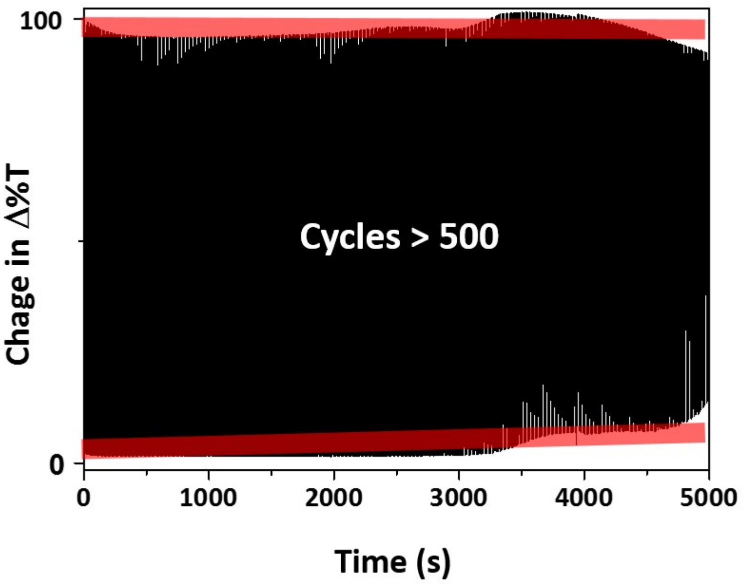

Fig. S4. Square-wave potential step absorptiometry of the ECW with PR-Br in BIL (monitored at 550 nm, -2.8 V to +2.8 V) for a **5 s**ec step for 5000 sec (500 cycles).

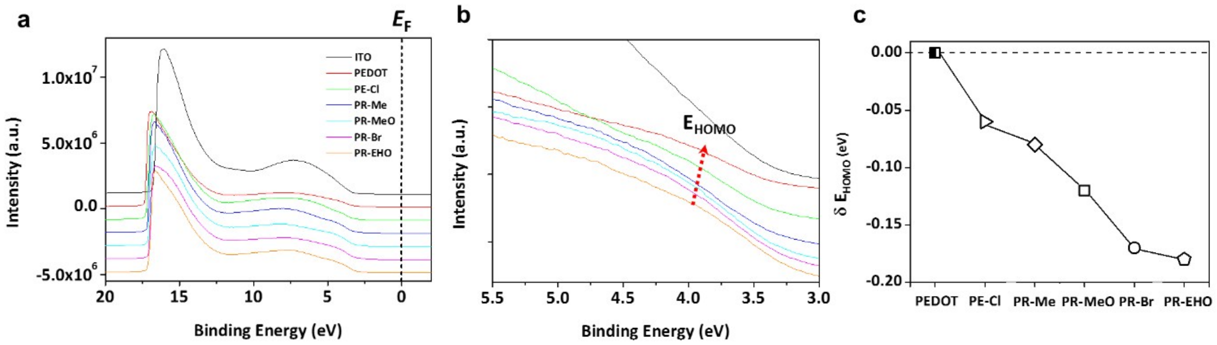

Fig. S5. (**a**) UPS spectra for the CPs on ITO using He(I) irradiation. (**b**) Magnified view of the Fermi-edge (dotted black line) and valence band state region. The x axis short solid line shows the binding energy relative to the *E*$_F$ of each material. (**c**) A plot of the HOMO edge (δE_{HOMO}) shift in referenced to PEDOT.

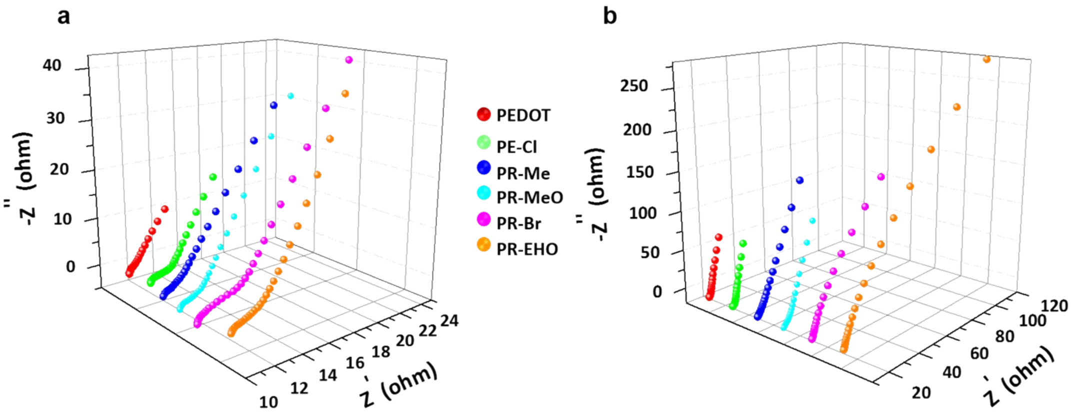

Fig. S6. Nyquist diagram of the electrochemical impedance spectra (EIS) at (**a**) the bleached state and (**b**) colored state. EIS conditions: frequency range: 100 kHz–48 Hz; signal amplitude: 20 mV; electrolyte: BIL.

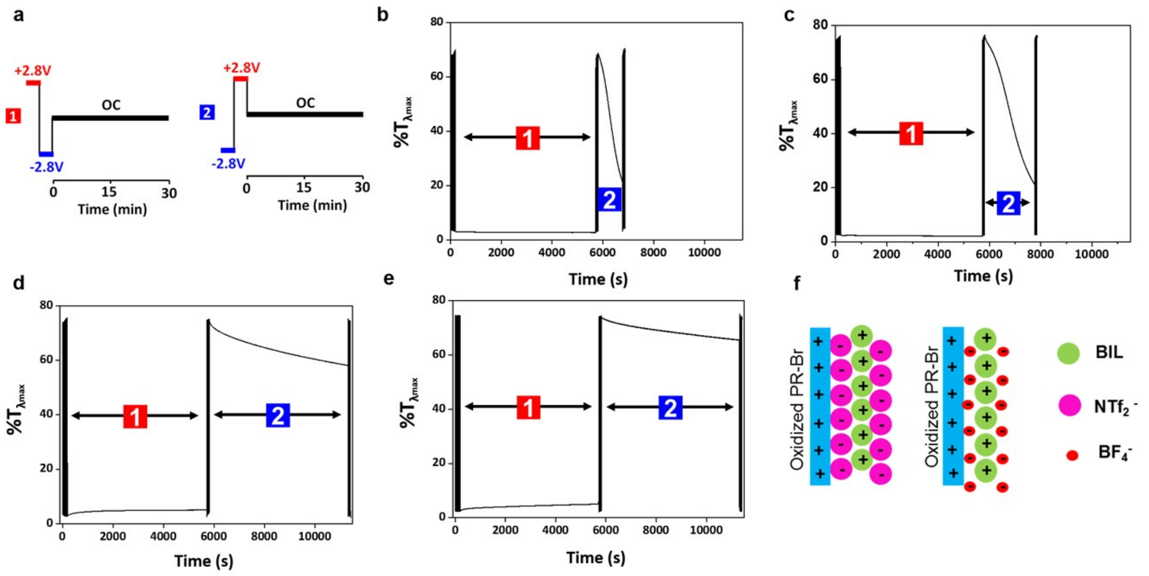

Fig. S7. (**a**) Repetitive step potentials given in the applied potential cycle. The OM of PR-Br ECW in different types of ILs. (**b**) BBF_4. (**c**) BMeS. (**d**) EIL. (**e**) BIL. (**f**) Schematic diagram for the electrochemical double layer having differnent anions in the ILs.

a

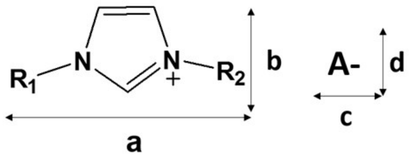

b

.	Cation					Anion		
	Name	R1	R2	Size (Å)		A-	Size (Å)	
				a	b		c	d
1	EIL	Ethyl	Methyl	7.55	4.24	bis(trifluoromethylsulfonyl)imide (NTf_2^-)	7.81	3.46
2	BIL	Butyl	Methyl	9.98	4.24	bis(trifluoromethylsulfonyl)imide(NTf_2^-)	7.81	3.46
3	BMeS	Butyl	Methyl	9.98	4.24	methyl sulfate (MeS)	5.04	3.15
4	BBF_4	Butyl	Methyl	9.98	4.24	Tetrafluoroborate (BF_4^-)	2.38	2.38

Fig. S8. (**a**) Chemical structure of the ILs and (**b**) approximate size (Å) of the cation and anion in the ILs calculated from the Gaussian program.

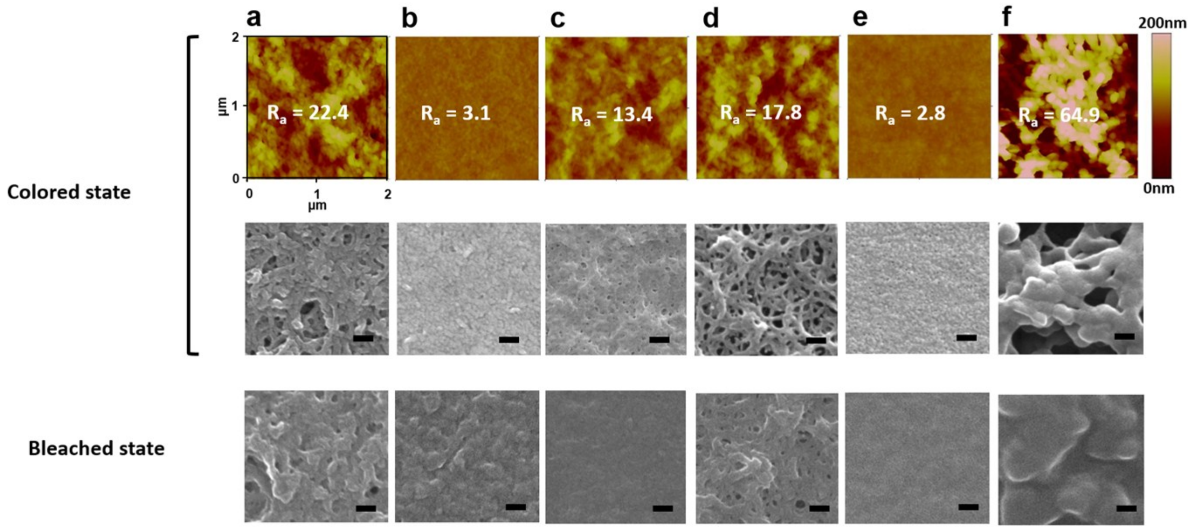

Fig. S9. The AFM and FE-SEM images (scale bars = 100 nm) of the CP films prepared via SCP at the colored states and bleached state. (**a**) PEDOT. (**b**) PE-Cl. (**c**) PR-Me. (**d**) PR-MeO. (**e**) PR-Br. (**f**) PR-EHO.

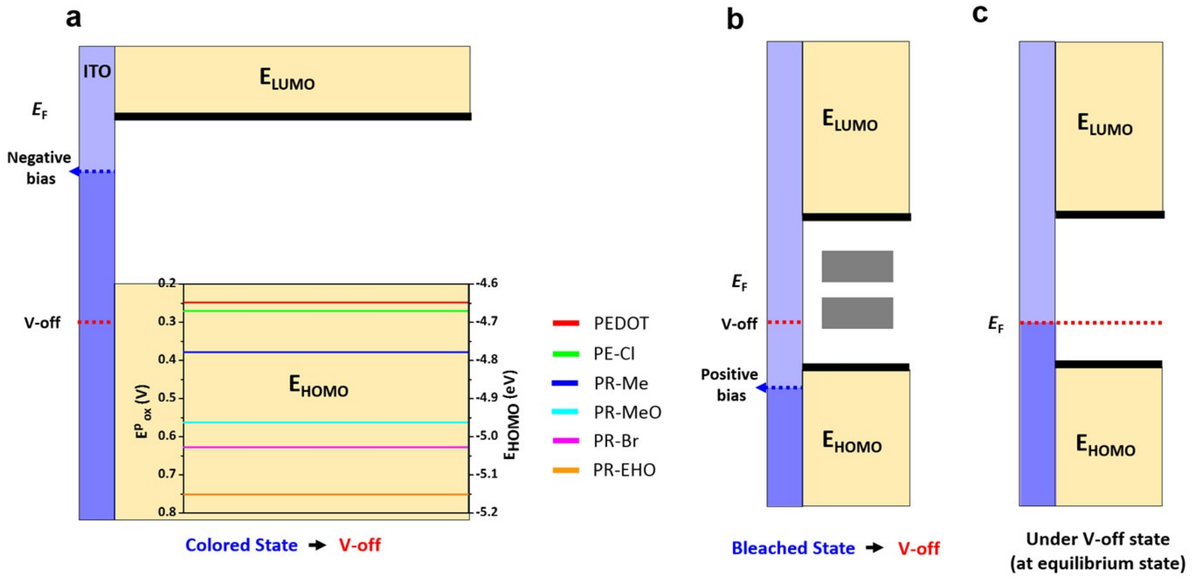

Fig. S10. Schematic illustration for the energy state of the CP in the (a) colored state, (b) bleached state and (c) equilibrium state

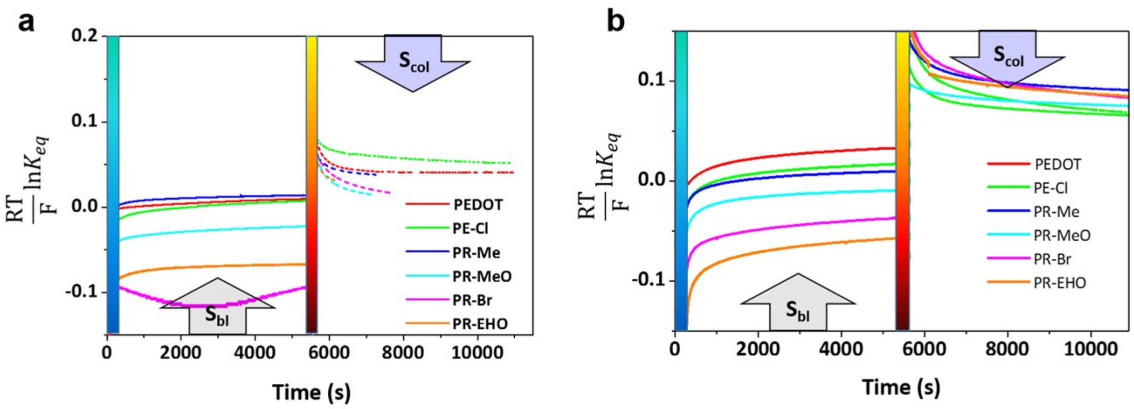

Fig. S11. A plot for the $\frac{RT}{F} lnK_{eq}$, obtained from the transmittance changes at V-off state, against V-off time for the ECWs in (**a**) TBAP and (**b**) BIL.

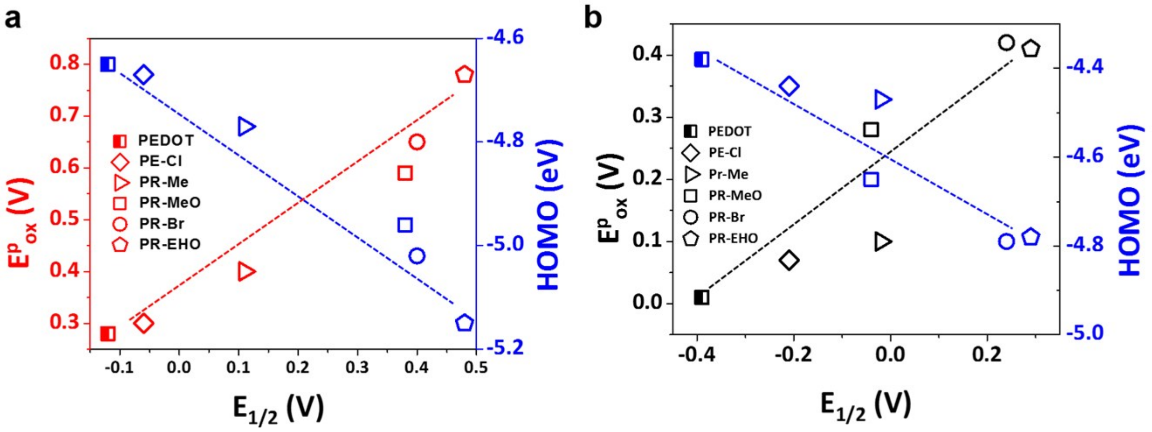

Fig. S12. A plot of the E^p_{ox} and E_{HOMO} as a function of $E_{1/2}$ in (**a**) TBAP and (**b**) BIL.

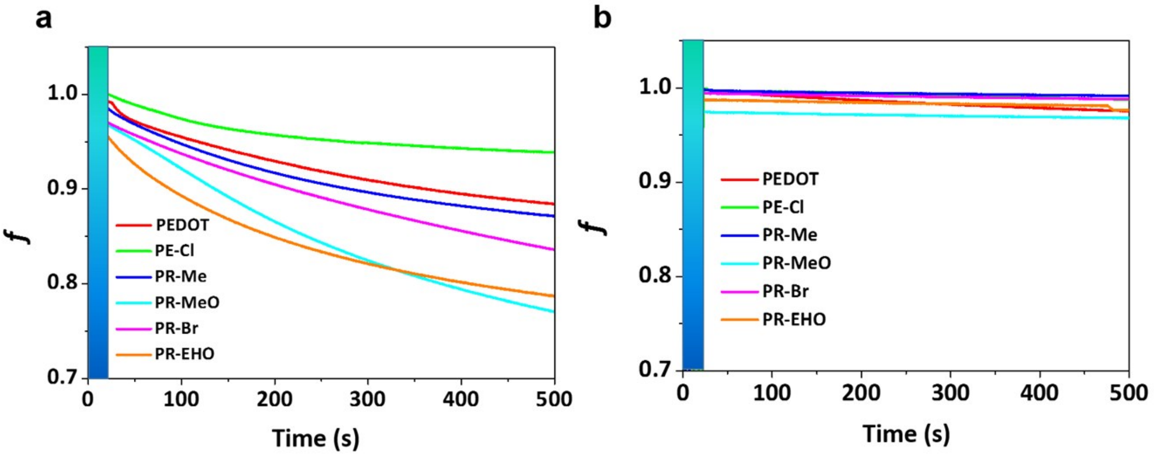

Fig. S13. In-situ *f* changes of the ECW with (**a**) TBAP and (**b**) BIL.

Table S1. Reduction and oxidation peak potentials of the CPs.

Electrolyte	TBAP					BIL				
CPs	E^{p}_{red1} [V][a]	$E^{p}_{,red2}$[V][b]	E^{p}_{ox1} [V][c]	E^{p}_{ox2} [V][d]	$E_{1/2}$ [V] [e]	E^{p}_{red1} [V]	$E^{p}_{,\,red2}$[V]	E^{p}_{ox1} [V]	E^{p}_{ox2} [V]	$E_{1/2}$ [V]
PEDOT	-0.52 (-0.53)	0.12	-0.34 (-0.33)	0.28 (0.27)	-0.12	-0.78 (-0.73)	-0.17	-0.51 (-0.53)	0.01 (0.02)	-0.39
PE-Cl	-0.42 (-0.4)	0.06 (0.10)	-0.12 (-0.11)	0.3 (0.25)	-0.06	-0.48 (-0.46)	-0.07 (-0.08)	-0.19	0.07 (0.09)	-0.21
PR-Me	-0.18 (0.01)	0.03	0.07	0.4 (0.35)	0.11	-0.14 (0.01)	0.06	-0.11	0.1 (0.1)	-0.02
PR-MeO	0.16 (0.17)	0.44 (0.41)	0.19 (0.18)	0.59 (0.54)	0.38	-0.36 (-0.27)	-0.04 (0.1)	-0.19 (-0.14)	0.28 (0.26)	-0.04
PR-Br	0.14 (0.27)	0.35	0.26	0.65 (0.63)	0.40	0.05 (0.21)	0.25	0.17	0.42 (0.48)	0.24
PR-EHO	0.17 (0.16)	0.35 (0.34)	0.58 (0.57)	0.78 (0.71)	0.48	0.17 (0.18)	0.25	0.26	0.41 (0.36)	0.29

The initial scan direction was toward a positive potential. [a] first E^{p}_{red}. [b] second E^{p}_{red} [c] first E^{p}_{ox}. [d] second E^{p}_{ox}, which were determined based on the Bigaussian multi-peak deconvolution of the cyclic voltammogram (the number in parenthesis indicates the reading value). [e] Half-wave potential ($E_{1/2} = (E^{p}_{red1} + E^{p}_{ox2})/2$).

Table S2. Electrochromic properties of the CPs in BIL.

CPs	Thickness (nm)	λ_{max} (nm)	Potential (V)	T_b [a] (%)	T_c [b] (%)	$\Delta\%T_{\lambda max}$ (%)	$\tau_{b0..95}$ [c] (S)	$\tau_{c0..95}$ [d] (S)	CE (cm^2/C)
PEDOT	160	610	±3.3	64	9	55(53)	0.7	2.9	183 (250[31])
PE-Cl	185	630	±3.3	71	3	68	0.7	2	303
PR-Me	175	578	±2.8	77	2	75 (70)	0.7	1.7	645 (580[31])
PR-MeO	190	576	±2.8	71	7	64	1.3	3.1	461
PR-Br	170	583	±2.8	74	2	72	1.5	0.7	879
PR-EHO	250	554	±2.8	82	16	66(65)	0.8	1.4	584 (1232[23])

[a] Transmittance of the 2-electrode ECW at the bleached state at a given wavelength for 5 sec. [b] Transmittance of the 2-electrode ECW at the colored state at a given wavelength for 5 sec. [c] The switching time required to reach 95% of the bleached state. [d] The switching time required to reach 95% of the colored state.

Table S3. Bistability of the CPs in TABP and BIL

Electrolyte	TBAP				BIL			
			Bistability ($\Delta\%T_{off}$)				Bistability ($\Delta\%T_{off}$)	
CPs	$\Delta\%T_{\lambda max}$ (%)	E_{HOMO} (eV)	Colored state (S_{bl}) [a]	Bleached state (S_{col}) [b]	$\Delta\%T_{\lambda max}$ (%)	E_{HOMO} (eV)	Colored state (S_{bl})	Bleached state (S_{col})
PEDOT	56	-4.65	18	17	55	-4.38	32	8
PE-Cl	68	-4.67	17	20	68	-4.44	22	12
PR-Me	74	-4.77	14	> 26 (12) [c]	75	-4.47	17	7
PR-MeO	62	-4.96	7	> 35 (30)	64	-4.65	12	5
PR-Br	71	-5.02	2	> 37 (33)	72	-4.79	2	9
PR-EHO	66	-5.15	1	> 47 (35)	66	-4.78	3	4

[a] $\Delta\%T_{oc}$ in the colored state after 90min [b] $\Delta\%T_{oc}$ in the bleached state after 90min [c] number in parenthesis indicates measurement time (min)

Table S4. The apparent rate constants (k_{app}).

k_{app}	PEDOT	PE-Cl	PR-Me	PR-MeO	PR-Br	PR-EHO
TBAP	- 5.22 x 10 - 3	- 3.54 x 10 - 3	- 6.48 x 10 - 3	- 1.17 x 10 - 2	- 7.74 x 10 - 3	- 9.50 x 10 - 3
BIL	- 1.35 x 10 - 3	- 7.03 x 10 - 4	- 3.50 x 10 - 4	- 3.75 x 10 - 4	- 3.60 x 10 - 4	- 3.74 x 10 - 4